

Anillin-related protein Mid1 regulates timely formation of the contractile ring in the fission yeast *Schizosaccharomyces japonicus*

Tsuyoshi Yasuda, Masak Takaine[§], Osamu Numata, and Kentaro Nakano*

Department of Biological Sciences, Graduate School of Life and Environmental Sciences,
University of Tsukuba, 1-1-1 Tennohdai, Tsukuba, Ibaraki 305-8572, Japan

[§]Present address: Gunma University Initiative for Advanced Research (GIAR), Gunma
University, 3-39-15 Showa-machi, Maebashi, Gunma 371-8512, Japan

Running title: Functional analysis of *S. japonicus* Mid1

*Corresponding to: Kentaro Nakano, Department of Biological Sciences, Graduate School
of Life and Environmental Sciences, University of Tsukuba, 1-1-1 Tennohdai, Tsukuba,
Ibaraki 305-8572, Japan

Tel: +81-29-853-6642

Fax: +81-29-853-6642

Email: knaknao@biol.tsukuba.ac.jp

Keywords: actin, cytokinesis, myosin, cell division

Abstract

In the fission yeast *Schizosaccharomyces pombe* (*Sp*), Mid1/Dmf1 plays an important role in positioning the division site by inducing formation of the contractile ring (CR). Mid1, emanating from the nucleus located in the cell center, forms a dozen of nodes in the middle cell cortex ahead of mitosis, and actin filaments and myosin II accumulated at each node interact and assemble the CR in metaphase. Curiously, in another fission yeast *S. japonicus* (*Sj*), CR formation begins after nuclear segregation in late anaphase. Here, we investigated the role of *S. japonicus* Mid1 during mitosis to compare the molecular mechanisms that determine the cell division site in *Schizosaccharomyces*. Similar to *Sp* Mid1, *Sj* Mid1 often accumulated in the nucleus of interphase cells. Moreover, *Sj* Mid1 localized to cortical dots with myosin II in the future division site and formed a medial ring in mitotic cells. However, *S. japonicus* cells without Mid1 function still performed symmetrical binary division. Therefore, the Mid1 dependency for positional control of the cell division site is possibly different between the two species. Meanwhile, we found that *Sj* Mid1 enhanced CR formation, in a manner possibly similar to that by *Sp* Mid1.

Introduction

During the contractile ring (CR)-dependent cytokinesis of eukaryotic cells, the interactions of filamentous actin (F-actin) and myosin II in the CR is thought to generate forces to constrict the cell body just beneath the cleavage furrow, enabling the mother cell to divide into two daughter cells. However, the molecular mechanism of the mitosis-specific assembly of F-actin and myosin II in CR formation at the proper region beneath the plasma membrane is not entirely clear.

The fission yeast *Schizosaccharomyces pombe* is an ideal organism to study the molecular mechanisms controlling CR formation during cytokinesis. In this organism, it has been revealed that the nucleocytoplasmic shuttling protein Mid1/Dmf1 plays a central role in the spatiotemporal control of CR formation (Chang *et al.* 1996, Sohrmann *et al.* 1996; Daga & Chang 2005; reviewed by Rincon & Paoletti 2012). Mid1 has a nuclear localization signal (NLS), a nuclear exclusion signal (NES), and an amphipathic sequence followed by a Pleckstrin-homology (PH) domain located at the C-terminus, which are considered important for its functions (Sohrmann *et al.* 1996; Paoletti & Chang 2000; Lee & Wu 2012). In interphase, most Mid1 is located in the nucleus but residual amounts of Mid1 form cortical dots called interphase nodes by interacting with the Cdr2 kinase and other proteins associated with the nodes (Almonacid *et al.* 2009; Rincon *et al.* 2014). The distribution of interphase nodes is restricted to the middle of the cell by exclusion from cell tips by the Pom1 kinase. As the G2 phase progress, the amount of Mid1 at the equatorial cortex, a region proximal to the nucleus positioning in the center of interphase cells, increases and other components such as Gef2, Blt1, and Klp8 localize to the interphase nodes (Moseley *et al.* 2009; Guzman-Vendrell *et al.* 2013; Akamatsu *et al.* 2014). Just after a cell enters mitosis, Cdr2 and other proteins are released from the interphase nodes and Mid1 and its associated proteins form cytokinetic nodes together with an IQGAP-like

protein Rng2, myosin II consisting of the heavy chain Myo2 and light chains Rlc1 and Cdc4, an F-BAR domain protein Cdc15, and formin Cdc12 (Wu *et al.* 2003, 2006; Vavylonis *et al.* 2008). The cytokinetic nodes induce a cortical actin-myosin meshwork encircling the future division site in the cell middle and are merged with each other. As a result, the CR is assembled before the onset of anaphase. In *S. pombe*, a gene disruption of *mid1*⁺ is lethal for cell proliferation at high temperatures and causes severe defects in the spatiotemporal control of CR formation. The position and orientation of the CR is frequently disturbed in *mid1* null cells (Sohrmann *et al.* 1996; Bähler *et al.* 1998a; Paoletti & Chang, 2000), and the timing of CR component accumulation is delayed in the mutants than that in the wild-type cells (Motegi *et al.* 2004; Hachet & Simanis 2008; Huang *et al.* 2008). Thus, Mid1 plays a central role in the spatiotemporal control of CR formation in *S. pombe*.

Mid1 has structural similarity to anillin, which plays an important role in animal cell cytokinesis (reviewed by D'Avianno 2009 and Piekny & Maddox 2010). Anillin functionally interacts with F-actin, myosin II, septin, and the plasma membrane under the control of Rho-type small GTPases to ensure cytokinesis progression (Oegema *et al.* 2000; Kinoshita *et al.* 2002; Straight *et al.* 2005; Hickson & O'Farrell 2008; Piekny & Glotzer 2008; Watanabe *et al.* 2010). Both Mid1 and anillin share a conserved sequence called an anillin-homology domain (AHD) that forms a C2 domain-like structure with a lipid-binding amphipathic region followed by a PH-domain at their C-termini (Sun *et al.* 2015). However, it is still unclear whether anillin and Mid1 share a common ancestral gene. Also, an orthologue of Mid1 has not been found in budding yeasts and filamentous fungi even though many of their genomes have been sequenced and annotated.

On the other hand, the genome of *S. pombe* contains *mid2*⁺, which encodes a protein that has an AHD and a PH-domain at its C-terminus and localizes to the cell division site

during cytokinesis (Berlin *et al.* 2003; Tasto *et al.* 2003). Moreover, Mid2 functionally interacts with the septin cytoskeleton (Berlin *et al.* 2003; Tasto *et al.* 2003; Martín-Cuadrado *et al.* 2005). Cells lacking *mid2*⁺ form a normal CR but have defective cell separation after cytokinesis in *S. pombe*. Importantly, *mid2*⁺ homologs are well conserved among yeasts and fungi (Sanders & Herskowits 1996; Gale *et al.* 2001; Berlin *et al.* 2003; Si *et al.* 2012). *BUD4* is one of them. This gene product controls bud site selection by interacting with the bud neck filaments consisted of septin in the budding yeast *Saccharomyces cerevisiae* (Sanders & Herskowits 1996; Gladfelter *et al.* 2005; Wu *et al.* 2015). In the filamentous fungus *Neurospora crassa*, the Bud4 homolog is required for the process of septum formation by interacting with the Rho-family small GTPases (Justa-Schuch *et al.* 2010; Delgado-Álvarez *et al.* 2014). The primary structure of Bud4 is more similar to *Sp* Mid2 than *Sp* Mid1 (Fig. S1). It is possible that *mid1*⁺ may have been derived from a *mid2*⁺ gene duplication event in *Schizosaccharomyces* after this group had branched off from other fungi.

Here, we investigated the role of Mid1 through the organization of F-actin and Rlc1, a light chain of myosin II, during CR formation in *Schizosaccharomyces japonicus*. This fission yeast is considered as the first to branch among the four *Schizosaccharomyces* species whose genomes have been sequenced (Rhind *et al.* 2011). Interestingly, pioneer work done by Alfa & Hyams (1990) demonstrated that an accumulation of F-actin in the equatorial region occurs during anaphase in *S. japonicus*. On the other hand, the CR is formed prior to the onset of anaphase in *S. pombe* as mentioned above. The discordance on the timing of CR formation between the two *Schizosaccharomyces* species may imply that the molecular mechanisms controlling CR formation differs between the two fission yeasts. Moreover, the function of Mid1 in controlling the organization of the CR in *S. japonicas* has not been explored until recently (Gu *et al.*, 2015). A gene manipulation technique that

has recently been established in *S. japonicus* (reviewed by Niki 2014) enabled us to study the function of Mid1 in this organism. In this manuscript, we report a comparative study of CR formation in *Schizosaccharomyces* species and address the functional significance of Mid1 during *S. japonicus* cytokinesis.

Results

***Sj* Mid1 localizes to the equatorial cell cortex and changes distribution from dots to a ring**

To study the cellular localization of *S. japonicus* Mid1 (*Sj* Mid1) by fluorescence microscopy, we prepared *S. japonicus* strains in which the gene for *mCherry* or *gfp* was introduced into an upstream position adjacent to the stop codon for *mid1*⁺ or *rlc1*⁺. A fluorescence-protein-fused myosin-regulatory light chain Rlc1 was a conventional marker protein to visualize CR dynamics in *S. pombe* (Le Goff *et al.* 2000; Naqvi *et al.* 2000; Wu *et al.* 2003). A cylindrically-shaped cell of fission yeast grows at the cell tip(s) and symmetrically divides into two daughter cells when the cell size reaches an appropriate length (Mitchison 1957; Mitchison & Nurse 1985). In relatively short cells presumed to be in interphase, we found that a significant fraction of *Sj* Mid1 localized with *Sj* Rlc1 in cortical dots at the mid region of cells (Fig. 1Aa, brackets), although only *Sj* Mid1 was detected in the nucleus (see below). Those dots may correspond to the interphase nodes of *S. pombe* (Paoletti & Chang 2000). Moreover, *Sj* Mid1-mCherry formed a medial ring encircling the cells containing CR (Fig. 1Aa, arrows). *Sj* Mid1 dots may narrow their distribution in *S. japonicus* similar to Mid1 behavior during metaphase in *S. pombe* (Sohrmann *et al.* 1996; Bähler *et al.* 1998; Paoletti & Chang 2000; Wu *et al.* 2003). A strain with a reciprocal combination of the fluorescently-tagged genes was also examined. Observing those cells with fluorescence microscopy, discontinuous filament-like structures in the cytoplasm were frequently observed using fluorescence microscopy with blue-light excitation for GFP (Fig. 1Ab). The same signal was also detected in wild-type cells not expressing a GFP construct (Fig. 1Ac), suggesting that the signal was autofluorescence presumably emanating from a cellular structure such as the mitochondria. Such autofluorescence was not detected in the confocal laser microscopy (Fig. 1B). In this strain,

Sj Mid1-GFP and *Sj* Rlc1-mCherry co-localized on a medial ring in elongated cells (Fig. 1Ab, arrows; Fig. 1B). However, *Sj* Mid1-GFP remained in a lateral region of septating cells, while a ring containing *Sj* Rlc1-mCherry, namely CR, was closing (Fig. 1Ab, arrowheads). The different behavior of these proteins was confirmed by time-lapse microscopy. After contraction of the Rlc1-mCherry ring had occurred, *Sj* Mid1-GFP remained on the cell cortex until the signal of *Sj* Mid1-GFP reached an undetectable level in late cytokinesis (Fig. 1C).

It has been reported that a large fraction of *Sp* Mid1 is sequestered in the interphase nucleus (Sohrmann *et al.* 1996; Bähler *et al.* 1998a; Paoletti & Chang 2000). Localization of *Sj* Mid1 in the nucleus was often observed in cells expressing Mid1-mCherry together with Cut11-GFP (Aoki *et al.* 2011) to visualize the nuclear envelope (Fig. 1Ad). In addition, we treated *S. japonicus* cells with leptomycin B (LMB), an inhibitor of nuclear export of NES-containing proteins (Nishi *et al.* 1994), and evaluated the nuclear accumulation of *Sj* Mid1. We found that cells showed nuclear localization of *Sj* Mid1 in an LMB-dependent manner (Fig. 2). Thus, *Sj* Mid1 may also shuttle between the nucleus and the cytoplasm in *S. japonicus* cells.

***Sj* Mid1 is not essential for vegetative cell growth**

To examine the functional importance of *Sj* Mid1 for cytokinesis in *S. japonicus*, the open reading frame of *mid1*⁺ was replaced with a *kanMX6* drug-resistance cassette by homologous recombination. The Δ *mid1*-null strain did not show defective in cell growth or morphology. Δ *mid1*-null cells were able to form colonies on a YE plate incubated at 16, 25, 30, 36 and 42°C similar to wild-type cells (Fig. 3A). Therefore, *Sj* Mid1 was dispensable for cell growth in *S. japonicus*. In addition, it appeared that the position of the septum in the cell body and cell separation after cytokinesis were unaffected in Δ *mid1*-null cells (Fig. 3B).

These data suggest that the dependency on Mid1 to position the cell division plane differs between *S. japonicus* and *S. pombe*, since a deletion of the *mid1*⁺ gene caused abnormal septum formation and temperature-sensitive growth defects in *S. pombe* (Sohrmann *et al.* 1996).

***Sj* Mid1 promotes myosin II and F-actin accumulation for CR formation**

To examine CR formation in $\Delta mid1$ -null cells, *Sj* Cut11-GFP and *Sj* Rlc1-mCherry were simultaneously introduced into the deletion strain. We noticed that the percentage of anaphase cells with *Sj* Rlc1-mCherry localization to the middle of the cell was lower in the $\Delta mid1$ strain compared to wild-type (Fig. 4A, B). *Sj* Rlc1-mCherry localized to the middle of the cell just prior to telophase and formed a ring, but its distribution was somewhat faint and uneven in $\Delta mid1$ -null cells (compare “cell 3” in $\Delta mid1$ with WT in Fig. 4A). Thus, these data suggest that *Sj* Mid1 might facilitate myosin II localization to the middle of the cell prior to cytokinesis and might be involved in the homogeneous distribution of myosin II in the CR during CR formation.

We further investigated the distribution of F-actin in $\Delta mid1$ -null cells. Previously, it has been shown that F-actin appears at the future division site after the onset of nuclear division in *S. japonicus* (Alfa & Hyams 1990). As shown in Fig. 4C, the CR tightly forms just prior to the completion of the segregation of daughter nuclear DNA in this organism. Remarkably, in a significant population of $\Delta mid1$ -null cells, F-actin accumulation was not detected in the middle of cells whose nuclear DNA had almost completely divided (“cell 2” indicated by a single asterisk in Fig. 4C; Fig. 4D). Moreover, F-actin was likely to have been loosely assembled into the CR in $\Delta mid1$ -null cells compared to wild-type cells (arrowheads in Fig. 4C). However, eventually, the F-actin seemed to be tightly arranged in the CR as telophase progressed (arrows in Fig. 4C), and CR constriction occurred (double

asterisk, Fig. 4C). We therefore conclude that the timing of myosin II and F-actin recruitment to form the CR in the future division site was significantly delayed in $\Delta mid1$ -null cells. Moreover, our observation of Rlc1-mCherry localization revealed that the distribution of myosin II in the early stages of CR formation appears to be quantitatively and qualitatively disturbed in the absence of *Sj* Mid1. Furthermore, we found that *Sj* Mid1 appears to facilitate the formation of a tightly packed F-actin ring prior to the onset of telophase. It is possible that *Sj* Mid1 may organize F-actin in the middle of the cell by controlling the distribution of myosin II. Alternatively, *Sj* Mid1 may induce actin-polymerization by interacting with actin-regulatory proteins other than myosin II, as discussed in detail below.

***S. japonicus* Mid1 fails to rescue the defects of an *S. pombe* Mid1 mutant**

While a gene disruption of *Sp mid1*⁺ dramatically affects CR formation in *S. pombe* (Sohrmann *et al.* 1996), fatal defects of CR formation was not occurred in *Sj mid1*-null cells of *S. japonicus*. The difference of Mid1 dependency on CR formation in the fission yeast species might result from poor conservation of Mid1 functional domains during evolution. We thus examined whether artificial expression of *Sj* Mid1 from the plasmid pREP1 (Maundrell 1993) could rescue the lethality of *S. pombe* $\Delta mid1$ -null cells at 36°C. We found that $\Delta mid1$ cells transformed with pREP1-HA *Sj* Mid1 did not grow at 36°C, a result similar to cells that were transformed with an empty vector control, while $\Delta mid1$ cells transformed with the control plasmid pREP1-HA-*Sp* Mid1 grew at 36°C (Fig. 5A). Thus, artificial expression of *Sj mid1*⁺ failed to complement the temperature-sensitive growth defect of *S. pombe* cells lacking endogenous *mid1*⁺. Meanwhile, we found that *Sp mid1*⁺ could not significantly complement a cellular function of *Sj mid1*⁺ (Fig. S2). Therefore, a gene function of *mid1*⁺ was not highly conserved in these fission yeast species.

We next investigated the cellular localization of *Sj* Mid1 in *S. pombe*. The protein motifs and domains required for the cellular localization of *Sp* Mid1 have been studied in detail (Paoletti & Chang 2000; Celton-Morizur *et al.* 2004; Almonacid *et al.* 2009 and 2011; Lee & Wu 2012; Saha & Pollard 2012b; Ye *et al.* 2012; Guzman-Vendrell *et al.* 2013; Rincon *et al.* 2014). Opposing activities of the NLS- and NES-motifs controls nucleocytoplasmic shuttling of *Sp* Mid1 (Paoletti & Chang 2000), and cytoplasmic Mid1 can relocate to the plasma membrane and interact with *Sp* Cdr2 via its central region to form nodes on the cell cortex around the nucleus positioned in the cell center (Almonacid *et al.* 2009; Lee & Wu 2012; Guzman-Vendrell *et al.* 2013; Rincon *et al.* 2014). The amphipathic region in AHD and the following C-terminal PH-domain are important for the membrane association of *Sp* Mid1 (Celton-Morizur *et al.* 2004; Almonacid *et al.* 2009; Lee & Wu 2012; Saha & Pollard 2012b; Guzman-Vendrell *et al.* 2013). Immediately after the G2/M transition, *Sp* Mid1 at the nodes recruits myosin II and CR-assembling proteins such as *Sp* Rng2 and *Sp* Cdc12, and the CR is formed by the interaction of F-actin with myosin II prior to the onset of chromosome segregation (Wu *et al.* 2003, 2006; Motegi *et al.* 2004). It has been demonstrated that the N-terminal half of *Sp* Mid1 can associate with the CR (Celton-Mozier *et al.* 2004; Almonacid *et al.* 2009; Saha & Pollard 2012b; Lee & Wu 2012; Guzman-Vendrell *et al.* 2013).

To explore which domain is less functionally conserved between *Sj* Mid1 and *Sp* Mid1, we transformed wild-type *S. pombe* cells with expression plasmids for YFP-fused *Sj* Mid1 or truncated mutant proteins. We found that YFP-*Sj* Mid1 did not localize to nodes or the CR in *S. pombe* cells (Fig. 5B). Instead, localization to membranous structures was seen. The membrane association of *Sj* Mid1 was probably exerted via its C-terminal region, since the N-terminal deletion mutant *Sj* Mid1 Δ N2 (592~954 a. a.) retained its membrane association, while the C-terminal half-deletion mutant *Sj* Mid1 Δ C1 (1~594 a. a.) failed to

localize to membranes. A significant portion of *Sj* Mid1 Δ C1 accumulated in a vacuole-like compartment. This truncated protein may be structurally disordered and brought in a vacuole. Meanwhile, *Sj* Mid1 Δ C2 (1~415 a. a.) did not associate with the CR whereas the corresponding domain of *Sp* Mid1 (1~420 a. a.) did (Lee & Wu 2012). Therefore, it was suggested that *Sj* Mid1 was unlikely to interact stably with CR components of *S. pombe*. On the other hand, *Sj* Mid1 Δ C2 showed a nuclear localization which was especially evident in interphase cells, suggesting that this region of Mid1 may be responsible for the nuclear localization of *Sj* Mid1. Coincidentally, N-terminal fragment of *Sp* Mid1 (150-308 a. a.) also localizes in the nucleus (Saha & Pollard 2012b), although the canonical NLS of *Sp* Mid1 was found in its C-terminal region (Paoletti & Chang 2000; Celton-Morizur *et al.* 2004; Almonacid *et al.* 2009). Therefore, an uncharacterized NLS may be located in the N-terminal half of Mid1 proteins (Fig. S3). Alternatively, Mid1 may also have NLS-independent nuclear localization activity.

Discussion

In this study, we demonstrated a functional role of Mid1 in *S. japonicus* cytokinesis. *Sj* Mid1 appeared as cortical dots with *Sj* Rlc1 in the middle region of interphase cells, and these proteins formed the medial ring in late anaphase (Fig. 1). As cytokinesis progressed, *Sj* Rlc1 localized to the contracting CR while *Sj* Mid1 remained at the cell periphery for a while and then disappeared from that location. This behavior of *Sj* Mid1 is reminiscent of Mid1 in *S. pombe* (Sohrmann *et al.* 1996; Paoletti & Chang 2000). *Sp* Mid1 plays a central role for determining the division plane prior to cytokinesis (Sohrmann *et al.* 1996; Paoletti & Chang 2000; Wu *et al.* 2003; Daga & Chang 2005). Nevertheless, we found that mitotic *S. japonicus* cells were able to divide into two cells with nearly equal sizes without *mid1*⁺ gene function (Fig. 3B), suggesting that the importance of Mid1 to spatiotemporally control cytokinesis is not conserved in these fission yeast species. Coincidentally, artificial expression of *Sj* Mid1 did not improve the temperature-sensitive cell growth of an *S. pombe* Δ *mid1* strain (Fig. 5A). The roles of Mid1 proteins in cytokinesis progression may have functionally diversified after the two species had evolutionally separated. While our manuscript was in preparation for submission, Gu and colleagues had independently reported the functional diversity of Mid1 proteins between *S. pombe* and *S. japonicus* (Gu *et al.* 2015). Their experimental results and ours agree with a few exceptions. In our study, it was originally demonstrated that *Sj* Mid1 enhanced the assembly of F-actin into the CR (Fig. 4D) and possessed a nuclear-localizing activity similarly to *Sp* Mid1 (Figs. 1, 2 and 5B). It is possible that the functional significance of Mid1 proteins in cytokinesis may have diverged in fission yeast species by using other proteins to control the spatiotemporal formation of the CR.

***Sj* Mid1 is required for the prompt CR formation**

It has been reported that CR formation is delayed in *S. pombe* when *mid1*⁺ gene function is removed (Motegi *et al.* 2004; Hachet & Simanis 2008; Huang *et al.* 2008). In those cells, CR components are assembled into a ring without intermediation of cortical nodes dependent on the SIN (septation initiation network)-signaling pathway (Hachet & Simanis 2008). On the other hand, CR formation occurs in anaphase in *S. japonicus* (Alfa & Hyams 1990). We found that a gene deletion of *Sj mid1*⁺ caused a delay in CR formation in *S. japonicus*. In those cells, the cortical localization of Rlc1 in the cell center is affected (Fig. 4A). It is possible that the timing of CR formation may be retarded due to a reduction in myosin II levels in the medial region. It has been demonstrated that Mid1 plays an important role for anchoring myosin II in the medial cortex together with Rng2 prior to CR formation in *S. pombe* (Motegi *et al.* 2004; Padmanabhan *et al.* 2011; Almonacid *et al.* 2011; Takaine *et al.* 2014). Similarly, *Sj* Mid1 may also contribute to CR formation by interacting with myosin II in *S. japonicus*. In addition, it is possible that the node-mediated Mid1 function may be exerted at nearly the same time as the activation of CR formation by SIN-dependent signaling in *S. japonicus*.

The process of CR formation in *S. pombe* has been well studied. Several minutes after the G2/M transition, Mid1 in nodes localizes myosin II to the cell center via interacting with Rng2 and induces actin polymerization from the nodes by recruiting a formin Cdc12 (Chang *et al.* 1997; Padmanabhan *et al.* 2011; Takaine *et al.* 2009, 2014; Laporte *et al.* 2011; Saha & Pollard 2012a). Myosin II and F-actin then interact with each other and CR formation rapidly progresses in metaphase (Motegi *et al.*, 2000; Wu *et al.* 2003). On the other hand, *Sj* Mid1 organized cortical dots containing Rlc1 before mitosis, but they stayed in the equatorial region without F-actin appearance until late anaphase. This is an interesting point that may possibly explain the difference in timing of CR formation between the two species. We consider two possibilities regarding the late CR formation in *S.*

japonicus. First, *Sj* Mid1 is possibly maintained in an inactive state and cannot promote actin polymerization until late anaphase. The other is that node-associated proteins, which induce CR formation such as Cdc12 may not be fully activated until late anaphase. Interestingly, it has been demonstrated that SIN-dependent phosphorylation releases Cdc12 from a semi-functional oligomer state to a fully-functional monomer state specifically in anaphase in *S. pombe* (Bohnert *et al.* 2013). Clarifying the function and regulation of the *S. japonicus* Cdc12 homolog may be important in determining the reason for the difference in CR formation timing in these fission yeast species.

Multiple molecular mechanisms exist to position the cell division site in fission yeast

In *S. pombe*, Mid1 is released from the nucleus, which is positioned at the cell center to the proximal cell cortex during G2 phase and forms nodes by interacting with Cdr2 and other functionally related proteins (Paoletti & Chang 2000; Wu *et al.* 2003, 2006; Almonacid *et al.* 2009; Guzman-Vendrell *et al.* 2013; Akamatsu *et al.* 2014; Rincon *et al.* 2014). Mid1-anchored nodes play critical roles for CR positioning in the cell center. Several mechanisms function cooperatively to ensure Mid1 localization to the middle cortex in *S. pombe*. The tip complex consisting of Tea1 with its associated proteins and Pom1 occlude Mid1 nodes from the cell tips (Padte *et al.* 2006; Celton-Morizur *et al.* 2006; Huang *et al.* 2007). Also, the cortical ER network retains Mid1 in the center of cells by restricting its diffusion (Zhang *et al.* 2010).

On the other hand, Mid1-independent mechanisms that position the CR in the cell middle or occlude CR formation at the cell tip may exist in *S. pombe*, although the molecular basis underlying these activities have not been fully uncovered (Huang *et al.* 2007; Padte *et al.* 2006, Rincon *et al.* 2014). It is possible that *S. japonicus* may mainly depend on Mid1-independent mechanisms for CR positioning. It has very recently been

reported that the Pom1 homolog in *S. japonicus* plays an important role for determining the division site via controlling the CR anchoring protein Cdc15 (Gu *et al.* 2015). In their paper, they showed that a gene deletion of *mid1*⁺ does not exacerbate the defect in CR positioning of *Δpom1*-null cells, suggesting that Mid1 possibly plays a minor role in positioning the cell division site as compared to Pom1 in *S. japonicus*. However, Pom1 is not essential for cell growth in *S. japonicus* (Gu *et al.* 2015). Therefore, it is possible that another pathway may also function to control the cell division site in *S. japonicus*.

The *mid1*⁺ gene might have been derived from *mid2*⁺ by gene duplication after the ancestor of *Schizosaccharomyces* branched from other taxa (*see* Introduction). Considering the phylogenetic relationship of fungi and yeasts, the Mid1-dependent system for positioning the division site may not be the most prominent mechanism. Molecular evolution studies demonstrated that *S. japonicus* is probably the earliest branched species of the fission yeasts (Rhind *et al.* 2011). It is therefore possible that *S. japonicus* may have some ancestral traits. As mentioned above, a recent study (Gu *et al.* 2015) is in agreement with our studies, which reveal that deletion of *mid1*⁺ did not cause a fatal defect in *S. japonicus* cytokinesis. It is possible that a dependency on Mid1 for cytokinesis may not have been required in this organism compared to *S. pombe*. Instead, ancestral spatiotemporal-controlling machinery may have a predominant function during cytokinesis in *S. japonicus*. Future studies comparing the molecular mechanism of cytokinesis between *S. pombe* and *S. japonicus* will shed light on how important mechanisms including nucleocytoplasmic shuttling of Mid1 for cell-division site positioning and the node-dependent spatiotemporal control system of CR formation have been established in the *Schizosaccharomyces* lineage.

Experimental procedures

Strains and handling of cells

S. pombe and *S. japonicus* strains used in this study are listed in Tables S1 and S2, respectively. Fundamental strains for launch of our work in cytokinesis of *S. japonicus* were kindly provided by Prof. H. Niki (National Institute of Genetics, Japan). We used the *NIG2028* strain as wild-type in this study according to pioneer work (Furuya & Niki 2009).

YE (0.5% Bacto yeast extract (Becton & Dickinson (BD)), 3% D-glucose (Wako), 2% Bacto agar (BD) for a plate) was used as the standard medium. Geneticin (G418; Sigma Aldrich or Alexis) was supplemented in YE plates at a final concentration of 100 $\mu\text{g/ml}$ to select for *KanMX6*-positive transformants. For microscopic observation, cells were cultured in YE liquid medium containing supplements including adenine, uracil, leucine, histidine, and lysine at final concentrations of 225 mg/L for each. For the same purpose, Edinburgh Minimal Media (EMM) (Forsburg & Rhind 2006) with supplements as mentioned above and SD (BD) was also used.

To establish an *S. japonicus* strain by making a genetic cross of parental strains, fresh colonies of parental strains grown on YE plates were mixed with a toothpick in a drop of sterilize water on an MEA plate (3% Bacto malt extract (BD), 2% Bacto agar (BD)). After incubation at 25°C for several days, spores derived from a mating parental strains were treated with β -glucuronidase (Sigma) for separating spores from each other by digesting asci. Then, spores were spread on a plate after a brief treatment with 30% ethanol to kill the parental cells. The descendant colonies were picked up and their genetic markers were tested.

Gene manipulation

All strains prepared in this study were constructed by homologous recombination of a

PCR-based altered gene with a target chromosomal gene using a set of pFA6a-kanMX6 series as a template (Bähler *et al.* 1998b).

To transform *S. japonicus* cells with the altered genes, an electroporation method was applied according to Aoki *et al.* (2010) as follows. *NIG2028* strain inoculated in 50 mL of YE liquid medium was incubated overnight at 30°C in a shaking bath to a 3×10^6 cells/mL cell density. Cells were isolated by centrifugation, and the resultant pellets were washed with 40 mL of ice-chilled MilliQ water three times. Cell pellets were suspended in 10 mL of 1 M sorbitol aqueous solution containing 50 mM dithiothreitol (DTT), and the suspension was shaken at 30°C for 15 min. After removing the supernatant by centrifugation, cells were suspended in 10 mL of 1 M sorbitol aqueous solution. Cells were centrifuged again and resuspended in 5 mL of 1 M sorbitol aqueous solution. This manipulation was repeated one more time, and cells were finally split into two 1.5 mL-microtubes. After gently pipetting cells with 5 μ L of 1 M sorbitol and 1 μ g transforming DNA, the microtubes were left on ice for 30 min. Electroporation was performed in a dedicated cuvette (gap distance, 2-mm) containing 40 μ L of the cell suspension with transforming DNA with the Genepulser II or Genepulser Xcell, the electroporation instruments of BioRad. Cells were perforated with a single electric pulse (200 Ω , 25 μ F, 2.3 kV, exponential) which allowed the DNA to be introduced into the cells. At once, a small amount of 1 M sorbitol aqueous solution was added to the cuvette and the suspension of cells was transferred into 5 mL YE medium supplemented with 40 μ g/mL adenine and 20 μ g/mL uracil (final concentration). After an overnight incubation at 30°C, the transformed cells were spread onto YE plates containing G418 (100 μ g/ml), adenine (40 μ g/mL), and uracil (20 μ g/mL)(YEAUG), and the plates were further incubated at the same temperature. After several days, colonies growing on the plate were selected and streaked onto a new YEAUG plate.

Transformation of *S. pombe* was performed mainly by the lithium acetate method (Okazaki *et al.* 1990). An electroporation method (Suga & Hatakeyama 2001) was also used in some cases.

Localization domain analysis

To observe the cellular localization of *Sj* Mid1 in *S. pombe*, *yfp* gene-fused *Sj mid1*⁺ cDNA was inserted between *Nde*I and *Sal*I in the multiple-cloning site of the pREP1-expression vector (Maundrell 1993). Subsequently, vectors for expression of various lengths of truncated *Sj* Mid1 were constructed using a PCR-based mutagenesis kit (Takara) using the following sets of oligo-nucleotides;

5'-TCTCGAGCGGCCGCCCTTGTACAGCTCGTCCAT-3' and
5'-GGCGGCCGCTCGAGAGACGAAGATGATAGC-3' for Δ N1,
5'-TCTCGAGCGGCCGCCCTTGTACAGCTCGTCCAT-3' and
5'-GGCGGCCGCTCGAGAGGCAAGCTTTATCTT-3' for Δ N2,
5'-TGACTGACTGACGATGTAAAAGGAATGTC-3' and
5'-ATCGTCAGTCAGTCAGCAAGGTGAAGATAA-3' for Δ C1, and
5'-TGACTGACTGACGATGTAAAAGGAATGTC-3' and
5'-ATCGTCAGTCAGTCATGTTACCGGCAGACA-3' for Δ C2. Wild-type cells transformed with the generated vectors were cultured in EMM medium at 25°C and observed under fluorescence microscopy.

Microscopy

Cells were photographed with the upright microscope BX51 (Olympus) equipped with the cooled charge-coupled device (CCD) camera ORCAII-ER-1394 (Hamamatsu photonics). Digital images were acquired with Simple PCI software (Compix Inc.).

For time-lapse observation of fluorescent protein-expressing cells, the inverted microscope BX71 (Olympus) equipped with the spinning disc confocal scanner unit CSU22 (Yokogawa) with 488 and 568 nm laser units, a piezo-actuator for Z-scanning (Physik), and the EM-CCD camera iXon3 885 (Andor) was used. The system was controlled by MetaMorph software (Molecular Devices). Cell cultures were mounted on glass slides, and the prepared slides were sealed with vacuum grease to avoid evaporation of water. Z-sectioning images were collected at 0.3 μm intervals. The acquired images were processed by ImageJ 1.43 software (Wayne Rasband, National Institutes of Health, USA).

Cell staining

Cell cultures were fixed with one-tenth volume of 30% formaldehyde-containing PEM buffer (0.1 M Pipes (pH 6.8), 1 mM EGTA, 1 mM MgCl_2). After 1 h, cells were washed with PEM buffer three times and were suspended in PEM buffer with 0.6 mg/mL of Zymolyase 100T (Seikagaku Co. Ltd.) for partial cell wall lysing. After 5 min, cells were gently resuspended in PEM buffer containing 1% Triton-X 100 and were washed with PEM buffer three times. To stain for F-actin, the perforated cells were treated with 0.15 U BODIPY-phalloidin (Invitrogen) for 1 h. After replacing the staining solution with PEM containing 4', 6-diamidino-2-phenylindole (DAPI), cells were observed with fluorescence microscopy.

Acknowledgements

We are deeply grateful to Prof. H. Niki & Dr. K. Aoki (National Institute of Genetics, Japan) for providing us *S. japonicus* strains and genetic materials and for valuable advice.

This work was supported by a Grant-in-Aid for Scientific Research to K. N. from the Ministry of Education, Culture, Sports, Science and Technology (MEXT) (No. 24570207).

References

- Akamatsu, M., Berro, J., Pu, K.M., Tebbs, I.R. & Pollard, T.D. (2014) Cytokinetic nodes in fission yeast arise from two distinct types of nodes that merge during interphase. *J. Cell Biol.* **204**, 977–988.
- Alfa, C.E. & Hyams, J.S. (1990) Distribution of tubulin and actin through the cell division cycle of the fission yeast *Schizosaccharomyces japonicus* var. *versatilis*: a comparison with *Schizosaccharomyces pombe*. *J. Cell. Sci.* **96 (Pt 1)**, 71–77.
- Almonacid, M., Moseley, J.B., Janvore, J., Mayeux, A., Fraissier, V., Nurse, P. & Paoletti, A. (2009) Spatial control of cytokinesis by Cdr2 kinase and Mid1/Anillin nuclear export. *Curr. Biol.* **19**, 961–966.
- Almonacid, M., Celton-Morizur, S., Jakubowski, J.L., Dingli, F., Loew, D., Mayeux, A., Chen, J.S., Gould, K.L., Clifford, D.M. & Paoletti, A. (2011). Temporal control of contractile ring assembly by Plo1 regulation of myosin II recruitment by Mid1/Anillin. *Curr. Biol.* **21**, 473–479.
- Aoki, K., Nakajima, R., Furuya, K. & Niki, H. (2010) Novel episomal vectors and a highly efficient transformation procedure for the fission yeast *Schizosaccharomyces japonicus*. *Yeast* **27**, 1049–1060.
- Aoki, K., Hayashi, H., Furuya, K., Sato, M., Takagi, T., Osumi, M., Kimura, A. & Niki, H. (2011) Breakage of the nuclear envelope by an extending mitotic nucleus occurs during anaphase in *Schizosaccharomyces japonicus*. *Genes Cells* **16**, 911–926.
- Bähler, J., Steever, A.B., Wheatley, S., Wang, Y. I, Pringle, J.R., Gould, K.L. & McCollum, D. (1998a) Role of polo kinase and Mid1p in determining the site of cell division in fission yeast. *J. Cell Biol.* **143**, 1603–1616.

Bähler, J., Wu, J.Q., Longtine, M.S., Shah, N.G., McKenzie, A.III, Steever, A.B., Wach, A., Philippsen, P. & Pringle, J.R. (1998b) Heterologous modules for efficient and versatile PCR-based gene targeting in *Schizosaccharomyces pombe*. *Yeast* **14**, 943–951.

Berlin, A., Paoletti, A. & Chang, F. (2003) Mid2p stabilizes septin rings during cytokinesis in fission yeast. *J. Cell Biol.* **160**, 1083–1092.

Bohnert, K.A., Grzegorzewska, A.P., Willet, A.H., Vander Kooi, C.W., Kovar, D.R. & Gould, K.L. (2013) SIN-dependent phosphoinhibition of formin multimerization controls fission yeast cytokinesis. *Genes Dev.* **27**, 2164–2177.

Celton-Morizur, S., Bordes, N., Fraissier, V., Tran, P.T. & Paoletti, A. (2004) C-terminal anchoring of mid1p to membranes stabilizes cytokinetic ring position in early mitosis in fission yeast. *Mol. Cell. Biol.* **24**, 10621–10635.

Celton-Morizur, S., Racine, V., Sibarita, J.B. & Paoletti, A. (2006) Pom1 kinase links division plane position to cell polarity by regulating Mid1p cortical distribution. *J. Cell. Sci.* **119**, 4710–4718.

Chang, F., Woollard, A. & Nurse, P. (1996) Isolation and characterization of fission yeast mutants defective in the assembly and placement of the contractile actin ring. *J. Cell. Sci.* **109**, 131–142.

Chang, F., Drubin, D. & Nurse, P. (1997). cdc12p, a protein required for cytokinesis in fission yeast, is a component of the cell division ring and interacts with profilin. *J. Cell Biol.* **137**, 169–182.

Daga, R.R. & Chang, F. (2005) Dynamic positioning of the fission yeast cell division plane. *Proc. Natl. Acad. Sci. U.S.A.* **102**, 8228–8232.

D’Avino, P.P. (2009) How to scaffold the contractile ring for a safe cytokinesis - lessons from Anillin-related proteins. *J. Cell. Sci.* **122**, 1071–1079.

- Delgado-Álvarez, D.L., Bartnicki-García, S., Seiler, S. & Mouriño-Pérez, R.R. (2014) Septum development in *Neurospora crassa*: the septal actomyosin tangle. *PLoS ONE* **9**, e96744.
- Forsburg, S.L. & Rhind, N. (2006) Basic methods for fission yeast. *Yeast* **23**, 173–183.
- Furuya, K. & Niki, H. (2009) Isolation of heterothallic haploid and auxotrophic mutants of *Schizosaccharomyces japonicus*. *Yeast* **26**, 221–233.
- Gale, C., Gerami-Nejad, M., McClellan, M., Vandoninck, S., Longtine, M.S. & Berman, J. (2001) *Candida albicans* Int1p interacts with the septin ring in yeast and hyphal cells. *Mol. Biol. Cell* **12**, 3538–3549.
- Gladfelter, A.S., Kozubowski, L., Zyla, T.R. & Lew, D.J. (2005) Interplay between septin organization, cell cycle and cell shape in yeast. *J. Cell. Sci.* **118**, 1617–1628.
- Gu, Y., Yam, C. & Oliferenko, S. (2015) Rewiring of cellular division site selection in evolution of fission yeasts. *Curr. Biol.* **25**, 1187–1194.
- Guzman-Vendrell, M., Baldissard, S., Almonacid, M., Mayeux, A., Paoletti, A. & Moseley, J.B. (2013) Blt1 and Mid1 provide overlapping membrane anchors to position the division plane in fission yeast. *Mol. Cell. Biol.* **33**, 418–428.
- Hachet, O. & Simanis, V. (2008) Mid1p/anillin and the septation initiation network orchestrate contractile ring assembly for cytokinesis. *Genes Dev.* **22**, 3205–3216.
- Hickson, G.R.X. & O'Farrell, P.H. (2008) Rho-dependent control of anillin behavior during cytokinesis. *J. Cell Biol.* **180**, 285–294.
- Huang, Y., Chew, T.G., Ge, W. & Balasubramanian, M.K. (2007) Polarity determinants Tea1p, Tea4p, and Pom1p inhibit division-septum assembly at cell ends in fission yeast. *Dev. Cell* **12**, 987–996.

- Huang, Y., Yan, H. & Balasubramanian, M.K. (2008) Assembly of normal actomyosin rings in the absence of Mid1p and cortical nodes in fission yeast. *J. Cell Biol.* **183**, 979–988.
- Justa-Schuch, D., Heilig, Y., Richthammer, C. & Seiler, S. (2010) Septum formation is regulated by the RHO4-specific exchange factors BUD3 and RGF3 and by the landmark protein BUD4 in *Neurospora crassa*. *Mol. Microbiol.* **76**, 220–235.
- Kinoshita, M., Field, C.M., Coughlin, M.L., Straight, A.F. & Mitchison, T.J. (2002) Self- and actin-templated assembly of mammalian septins. *Dev. Cell* **3**, 791–802.
- Laporte, D., Coffman, V.C., Lee, I.J. & Wu, J.Q. (2011) Assembly and architecture of precursor nodes during fission yeast cytokinesis. *J. Cell Biol.* **192**, 1005–1021.
- Lee, I.J. & Wu, J.Q. (2012) Characterization of Mid1 domains for targeting and scaffolding in fission yeast cytokinesis. *J. Cell. Sci.* **125**, 2973–2985.
- Le Goff, X., Motegi, F., Salimova, E., Mabuchi, I. & Simanis, V. (2000) The *S. pombe rlc1* gene encodes a putative myosin regulatory light chain that binds the type II myosins myo3p and myo2p. *J. Cell. Sci.* **113 Pt 23**, 4157–4163.
- Martín-Cuadrado, A.B., Morrell, J.L., Konomi, M., An, H., Petit, C., Osumi, M., Balasubramanian, M., Gould, K.L., del Rey, F. & de Aldana, C.R.V. (2005) Role of septins and the exocyst complex in the function of hydrolytic enzymes responsible for fission yeast cell separation. *Mol. Biol. Cell* **16**, 4867–4881.
- Maundrell, K. (1993) Thiamine-repressible expression vectors pREP and pRIP for fission yeast. *Gene* **123**, 127–130.
- Mitchison, J.M. (1957) The growth of single cells. I. *Schizosaccharomyces pombe*. *Exp. Cell Res.* **13**, 244–262.
- Mitchison, J.M. & Nurse, P. (1985) Growth in cell length in the fission yeast *Schizosaccharomyces pombe*. *J. Cell. Sci.* **75**, 357–376.

Moseley, J.B., Mayeux, A., Paoletti, A. & Nurse, P. (2009) A spatial gradient coordinates cell size and mitotic entry in fission yeast. *Nature* **459**, 857–860.

Motegi, F., Mishra, M., Balasubramanian, M.K. & Mabuchi, I. (2004) Myosin-II reorganization during mitosis is controlled temporally by its dephosphorylation and spatially by Mid1 in fission yeast. *J. Cell Biol.* **165**, 685–695.

Naqvi, N.I., Wong, K.C.Y., Tang, X. & Balasubramanian, M.K. (2000) Type II myosin regulatory light chain relieves auto-inhibition of myosin-heavy-chain function. *Nat. Cell Biol.* **2**, 855–858.

Niki, H. (2014) *Schizosaccharomyces japonicus*: the fission yeast is a fusion of yeast and hyphae. *Yeast* **31**, 83–90.

Nishi, K., Yoshida, M., Fujiwara, D., Nishikawa, M., Horinouchi, S. & Beppu, T. (1994) Leptomycin B targets a regulatory cascade of crm1, a fission yeast nuclear protein, involved in control of higher order chromosome structure and gene expression. *J. Biol. Chem.* **269**, 6320–6324.

Oegema, K., Savoian, M.S., Mitchison, T.J. & Field, C.M. (2000) Functional analysis of a human homologue of the *Drosophila* actin binding protein anillin suggests a role in cytokinesis. *J. Cell Biol.* **150**, 539–552.

Okazaki, K., Okazaki, N., Kume, K., Jinno, S., Tanaka, K. & Okayama, H. (1990) High-frequency transformation method and library transducing vectors for cloning mammalian cDNAs by trans-complementation of *Schizosaccharomyces pombe*. *Nucleic Acids Res.* **18**, 6485–6489.

Padmanabhan, A., Bakka, K., Sevugan, M., Naqvi, N.I., D'souza, V., Tang, X., Mishra, M. & Balasubramanian, M.K. (2011) IQGAP-related Rng2p organizes cortical nodes and ensures position of cell division in fission yeast. *Curr. Biol.* **21**, 467–472.

- Padte, N.N., Martin, S.G., Howard, M. & Chang, F. (2006) The cell-end factor Pom1p inhibits Mid1p in specification of the cell division plane in fission yeast. *Curr. Biol.* **16**, 2480–2487.
- Paoletti, A. & Chang, F. (2000) Analysis of mid1p, a protein required for placement of the cell division site, reveals a link between the nucleus and the cell surface in fission yeast. *Mol. Biol. Cell* **11**, 2757–2773.
- Piekny, A.J. & Glotzer, M. (2008) Anillin is a scaffold protein that links RhoA, actin, and myosin during cytokinesis. *Curr. Biol.* **18**, 30–36.
- Piekny, A.J. & Maddox, A.S. (2010). The myriad roles of Anillin during cytokinesis. *Semin. Cell Dev. Biol.* **21**, 881–891.
- Rhind, N., Chen, Z., Yassour, M. *et al.* (2011) Comparative functional genomics of the fission yeasts. *Science* **332**, 930–936.
- Rincon, S.A. & Paoletti, A. (2012) Mid1/anillin and the spatial regulation of cytokinesis in fission yeast. *Cytoskeleton* **69**, 764–777.
- Rincon, S.A., Bhatia, P., Bicho, C., Guzman-Vendrell, M., Fraiser, V., Borek, W.E., Alves, F.d.L., Dingli, F., Loew, D., Rappsilber, J., Sawin, K.E., Martin, S.G. & Paoletti, A. (2014) Pom1 regulates the assembly of Cdr2-Mid1 cortical nodes for robust spatial control of cytokinesis. *J. Cell Biol.* **206**, 61–77.
- Saha, S. & Pollard, T.D. (2012a) Anillin-related protein Mid1p coordinates the assembly of the cytokinetic contractile ring in fission yeast. *Mol. Biol. Cell* **23**, 3982–3992.
- Saha, S. & Pollard, T.D. (2012b) Characterization of structural and functional domains of the anillin-related protein Mid1p that contribute to cytokinesis in fission yeast. *Mol. Biol. Cell* **23**, 3993–4007.

- Sanders, S.L. & Herskowitz, I. (1996) The BUD4 protein of yeast, required for axial budding, is localized to the mother/BUD neck in a cell cycle-dependent manner. *J. Cell Biol.* **134**, 413–427.
- Si, H., Rittenour, W.R., Xu, K., Nicksarlian, M., Calvo, A.M. & Harris, S.D. (2012) Morphogenetic and developmental functions of the *Aspergillus nidulans* homologues of the yeast bud site selection proteins Bud4 and Axl2. *Mol. Microbiol.* **85**, 252–270.
- Sohrmann, M., Fankhauser, C., Brodbeck, C. & Simanis, V. (1996) The *dmf1/mid1* gene is essential for correct positioning of the division septum in fission yeast. *Genes Dev.* **10**, 2707–2719.
- Straight, A.F., Field, C.M. & Mitchison, T.J. (2005) Anillin binds nonmuscle Myosin II and regulates the contractile ring. *Mol. Biol. Cell* **16**, 193–201.
- Suga, M. & Hatakeyama, T. (2001) High efficiency transformation of *Schizosaccharomyces pombe* pretreated with thiol compounds by electroporation. *Yeast* **18**, 1015–1021.
- Sun, L., Guan, R., Lee, I.J., Liu, Y., Chen, M., Wang, J., Wu, J.Q. & Chen, Z. (2015) Mechanistic insights into the anchorage of the contractile ring by Anillin and Mid1. *Dev. Cell* **33**, 413–426.
- Takaine, M., Numata, O. & Nakano, K. (2009) Fission yeast IQGAP arranges actin filaments into the cytokinetic contractile ring. *EMBO J.* **28**, 3117–3131.
- Takaine, M., Numata, O. & Nakano, K. (2014) Fission yeast IQGAP maintains F-actin-independent localization of myosin-II in the contractile ring. *Genes Cells* **19**, 161–176.
- Tasto, J.J., Morrell, J.L. & Gould, K.L. (2003) An anillin homologue, Mid2p, acts during fission yeast cytokinesis to organize the septin ring and promote cell separation. *J. Cell Biol.* **160**, 1093–1103.

Vavylonis, D., Wu, J.Q., Hao, S., O'Shaughnessy, B. & Pollard, T.D. (2008) Assembly mechanism of the contractile ring for cytokinesis by fission yeast. *Science* **319**, 97–100.

Watanabe, S., Okawa, K., Miki, T., Sakamoto, S., Morinaga, T., Segawa, K., Arakawa, T., Kinoshita, M., Ishizaki, T. & Narumiya, S. (2010) Rho and Anillin-dependent control of mDia2 localization and function in cytokinesis. *Mol. Biol. Cell* **21**, 3193–3204.

Wu, J.Q., Kuhn, J.R., Kovar, D.R. & Pollard, T.D. (2003) Spatial and temporal pathway for assembly and constriction of the contractile ring in fission yeast cytokinesis. *Dev. Cell* **5**, 723–734.

Wu, J.Q., Sirotkin, V., Kovar, D.R., Lord, M., Beltzner, C.C., Kuhn, J.R. & Pollard, T.D. (2006) Assembly of the cytokinetic contractile ring from a broad band of nodes in fission yeast. *J. Cell Biol.* **174**, 391–402.

Wu, H., Guo, J., Zhou, Y.T. & Gao, X.D. (2015) The anillin-related region of Bud4 is the major functional determinant for Bud4's function in septin organization during bud growth and axial bud site selection in budding yeast. *Eukaryotic Cell* **14**, 241–251.

Ye, Y., Lee, I.J., Runge, K.W. & Wu, J.Q. (2012) Roles of putative Rho-GEF Gef2 in division-site positioning and contractile-ring function in fission yeast cytokinesis. *Mol. Biol. Cell* **23**, 1181–1195.

Zhang, D., Vjestica, A. & Oliferenko, S. (2010) The cortical ER network limits the permissive zone for actomyosin ring assembly. *Curr. Biol.* **20**, 1029–1034.

Figure legends

Fig. 1 *Sj* Mid1 localizes to the equatorial region of the cell cortex

(A) *JK133* (*mid1-mCherry rlc1-GFP*)(a) and *JK113* (*mid1-GFP rlc1-mCherry*)(b) were observed. Cells were logarithmically grown in EMM at 25°C. Bright-field image (BF; left) and inverted fluorescence images (middle and right) are shown. The bottom panels of (a) show magnified images of the trunk region of the cell indicated by large arrowhead (Bar, 2 μm). Mid1 often localized with Rlc1 in cortical dot(s) in the middle of cells with a relatively short cell length (brackets), while both proteins form a medial ring in cells fully elongated. Arrows indicate a cross-section of the Mid1 ring. After the onset of CR constriction, the signals deriving from the proteins separated; *Sj* Mid1 remained in the medial cortex (small arrowheads) while *Sj* Rlc1 associated with the CR. Five dividing cells (cells numbered 1~5) and one interphase cell (cell 6) are shown in (b). The numbers are related to the progression of the cell-division stage. The discontinuous filament-like signal in the cells shown in the middle panel of (b) is autofluorescence possibly from mitochondria, since the same pattern of signal is detected in wild-type strains not possessing any *gfp*-gene construct (c) by the same exposure condition as in (b). Note that the similar pattern is found in the Rlc1-GFP panel in (a) though the signal is faint because of the short time exposure. (d) *JK92* strain (*mid1-mCherry cut11-GFP*) was observed. Asterisk indicates a septate cell. (B) Three-dimensional reconstruction image of *JK113* cells. Z sectioned images (0.3 μm interval) were reconstructed by maximum projection (upper) and are rotated (70°) around the X-axis (bottom). Note that Mid1 and Rlc1 form the medial ring. (C) Time-lapse observation of *JK113* cells. Three-dimensional images reconstructed by maximum projection are shown. Mid1-GFP and Rlc1-mCherry localized together to cortical dots prior to formation of the medial ring (cell 1 and cell 2 at time 0). Within approximately ten minutes after both proteins had formed the medial ring (arrows),

contraction of the CR occurred as judged by the behavior of Rlc1-mCherry. On the other hand, Mid1-GFP remained at the cell cortex after the CR began constricting as indicated by arrowheads, and those signals gradually disappeared from the medial region (cell 1, 33-42 min; cell 2, 42-45 min; cell 3, 6-15 min). Bars, 10 μ m.

Fig. 2 Nuclear localization of *Sj* Mid1 is enhanced by LMB-treatment

S. japonicus cells expressing Mid1-mCherry (*JK30*) and Rlc1-mCherry (*JK31*) were treated with leptomycin B (LMB) at a final concentration of 100 μ g/ml for 2 h. Hoechst 33342 was applied to visualize nuclear DNA and septum. Inverted fluorescence images are shown. Panels in the top row show control cells treated with vehicle (ethanol) for the same period of time. Arrowheads indicate nuclear accumulation of *Sj* Mid1-mCherry. Note that LMB treatment induces abnormal condensation of nuclear DNA. No accumulation of *Sj* Rlc1-mCherry was found in the presence or absence of LMB. Bar, 10 μ m.

Fig. 3 *Sj* Mid1 is not essential for cell proliferation

(A) Wild-type (WT; *NIG2028*) and Δ *mid1* (*JK105*) cells were spread on YE plates and incubated at the indicated temperatures for 3 days. Incubation of a plate at 16°C was for 1 month. No significant difference in cell growth was found between the strains under any condition. (B) Bright-field images of WT and Δ *mid1* cells incubated overnight in YE liquid medium at the indicated temperatures. Chain-like cells not separated after cytokinesis were occasionally found in WT and Δ *mid1* cells (arrows), but their frequency was not significantly different between the two strains. Bar, 10 μ m.

Fig. 4 Effects of gene disruption of *mid1*⁺ on CR formation

(A) Cortical accumulation of Rlc1 at the cell center is affected in *Δmid1* cells. WT (*JK94*) and *Δmid1* (*JK148*) cells expressing Rlc1-mCherry and Cut11-GFP, as a nuclear marker, were grown in EMM at 25°C. “Cell 1” is in interphase. “Cell 2” is at the onset of nuclear division in early anaphase. “Cell 3” is probably just after anaphase or telophase onset. In WT cells, Rlc1 accumulates as cortical dots in the mid region in early anaphase, and Rlc1 is merged into the CR before the onset of cytokinesis. On the other hand, Rlc1 distribution is considerably affected in *Δmid1* cells. Brackets indicate Rlc1 accumulation in the mid region. Asterisk indicates a cell that has almost completed septum formation. (B) Quantification of Rlc1 localization patterns in mitotic cells. Cells incubated as in A were classified. At least 100 cells were counted at each stage. Average percentage from two independent experiments was shown. (C) F-actin distribution was compared in WT (*NIG2028*) and *Δmid1* (*JK105*) cells. Cells logarithmically growing at 25°C in YE were fixed and processed for visualizing DNA and F-actin. “Cell 1” is before mitosis. “Cell 2” is in late anaphase judging from condensed nuclear DNA. Single asterisks indicate *Δmid1* cells with no F-actin distribution in the cell center even at this stage. “Cell 3” is probably just after anaphase or in early telophase. Although “cell 3” of both strains form an F-actin ring in the cell center, the ring appeared fragile in *Δmid1* cells compared to WT (arrowheads). As telophase progressed, the F-actin ring tightly formed even in *Δmid1* cells (arrows) as well as in WT cells. Double asterisk indicates *Δmid1* cells having a fully formed septum in position. Actin dots were distributed on both sides of the septum in this cell. (D) Quantification of the number of cells showing F-actin distribution in the mid region in anaphase and telophase. Cells processed as in C were examined. At least 100 cells were counted at each stage. Average percentage with standard deviation from three independent experiments was shown. *T-test was performed.

Fig. 5 Examination of the functional conservation of Mid1 in fission yeast species

(A) Expression of *Sj* Mid1 was not able to complement the temperature-sensitive growth defect of an *S. pombe* $\Delta mid1$ strain. *S. pombe* $\Delta mid1$ cells transformed with pREP1 expressing HA-tagged proteins were streaked on SD plates, respectively. Cells were incubated at the indicated temperatures for 3 days. (B) Localization of YFP-fused *Sj* Mid1 and the truncated proteins in *S. pombe* cells. Wild-type *S. pombe* cells transformed with pREP1 containing YFP-*Sj mid1*⁺ gene and deletion mutants were incubated in EMM without thiamine for 20 h at 25°C to induce expression of the inserted gene. Nuclear- and vacuolar-localization of YFP-fused proteins were indicated by arrowheads and arrows, respectively.

Supplementary materials

Fig. S1 Phylogenetic tree of anillin-like proteins

The deduced amino acid sequences of the gene products indicated were analyzed by the Maximum-likelihood method (Felsenstein 1981). MEGA6 (Tamura *et al.* 2013) was used for alignment and phylogenetic tree construction. Each protein ID is as follows: *S. pombe* Mid1, NP_588075; *S. japonicus* Mid1, XP_002172396; *S. octosporus* Mid1, XP_013019560; *S. cryophilus* Mid1, XP_013024513; *S. pombe* Mid2, NP_594704; *S. japonicus* Mid2, XP_002171416; *S. octosporus* Mid2, XP_013018812; *S. cryophilus* Mid2, XP_013024814; *Homo sapiens* anillin, NP_001271230; *Neurospora crassa* BUD4, XP_011393771; *Candida albicans* INT1, KHC75147; *Saccharomyces cerevisiae* BUD4, NP_012625.

References

Felsenstein, J. (1981) Evolutionary trees from DNA sequences: a maximum likelihood approach. *J. Mol. Evol.* **17**, 368–376.

Tamura, K., Stecher, G., Peterson, D., Filipowski, A. & Kumar, S. (2013) MEGA6: Molecular Evolutionary Genetics Analysis version 6.0. *Mol. Biol. Evol.* **30**, 2725–2729.

Fig. S2 Gene complement test of *Sp midI*⁺ for *Sj midI*⁺

(A) A diagram of construction of *S. japonicus* strains prepared for this test. DNA fragments used for transformation of an *S. japonicus* wild-type strain are shown in the left. Plasmids used for the construction of them are shown in the right. To ligate each DNA fragments, *Nde*I- and *Spe*I-restriction sites were artificially introduced into *Sj midI*⁺ and *Sp midI*⁺, respectively. Amino acid sequence of the protein was not changed by the base substitution in both genes. (B) Cortical accumulation of Rlc1 at the cell center does not normally proceed in *S. japonicus* cells whose *Sj midI*⁺ was replaced by *Sp midI*⁺. Cells expressing

Rlc1-mCherry and Sad1-mCherry were grown in YE at 25°C and were examined as in Fig. 4B. At least 100 cells were counted at each stage. Average percentage from two independent experiments was shown. (C) F-actin distribution was compared in WT (*NIG2028*), *Δmid1::HA-Sj mid1-GFP* (*JK387*), *Δmid1::HA-Sp mid1-GFP* (*JK392*), and *Δmid1* (*JK105*) cells. Cells logarithmically growing at 25°C in YE were fixed and processed for visualizing DNA and F-actin. Quantification of the number of cells showing F-actin distribution in the mid region in anaphase and telophase was graphed as in Fig. 4D. At least 100 cells were counted at each stage. Average percentage with standard deviation from two independent experiments was shown. *T-test was performed.

Fig. S3 Schematic diagram of *Sp* Mid1 and *Sj* Mid1

According to Gu et al. (2015), NLS of *Sj* Mid1 seems to be less conserved.

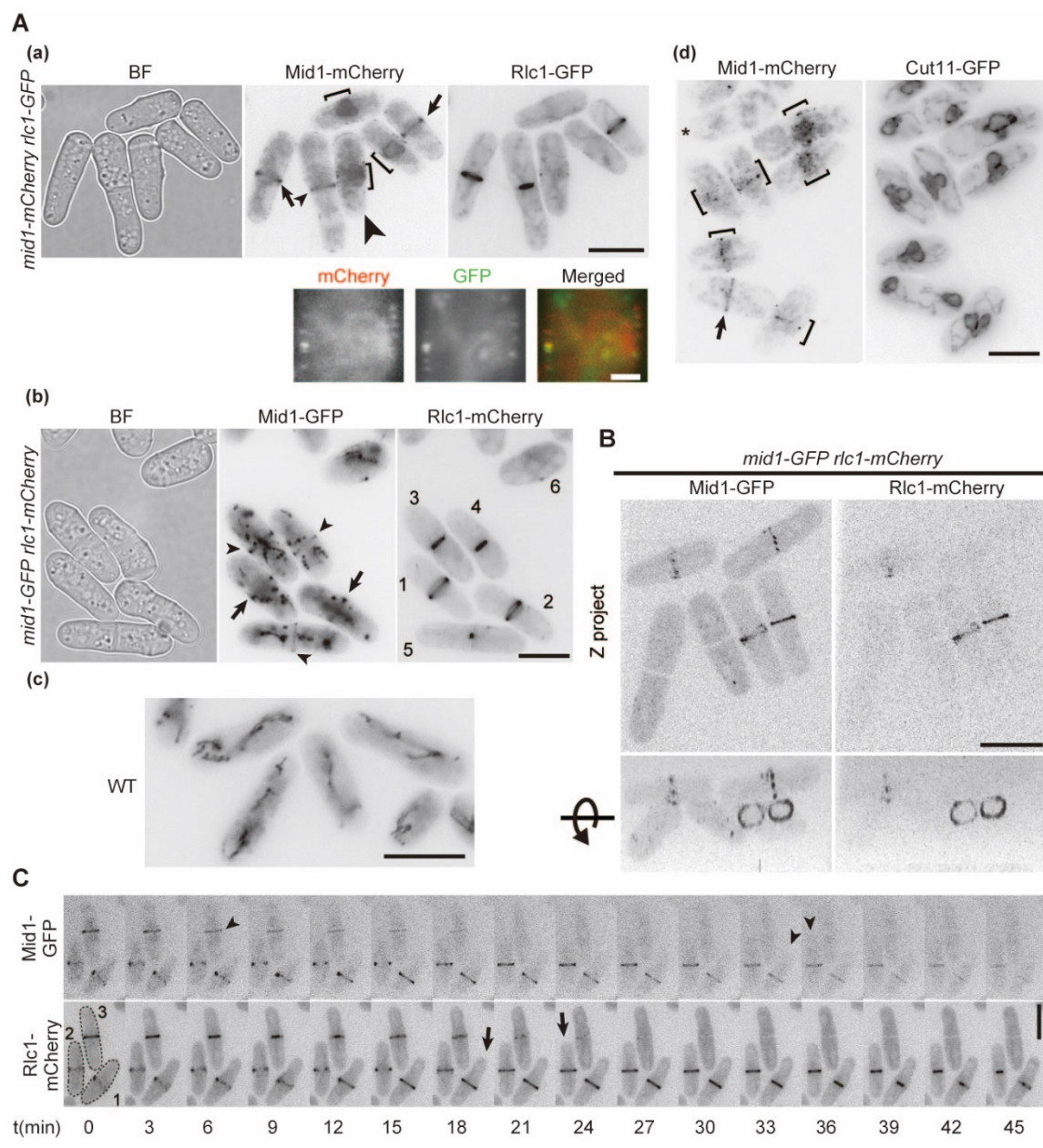
Table S1. *Schizosaccharomyces pombe* strains used in this study

strains	genotype	source
<i>JK1</i>	<i>h leu1-32</i>	Lab stock
<i>JK7</i>	<i>h leu1-32 ura4-D18 Δmid1::ura4⁺ pREP1-HA-Sp Mid1</i>	This study
<i>JK9</i>	<i>h leu1-32 ura4-D18 Δmid1::ura4⁺ pREP1-HA-Sj Mid1</i>	This study
<i>JK11</i>	<i>h leu1-32 ura4-D18 Δmid1::ura4⁺ pREP1-HA</i>	This study
<i>JK220</i>	<i>h leu1-32 pREP1-YFP-Sj Mid1 ΔC2</i>	This study
<i>JK234</i>	<i>h leu1-32 pREP1-YFP-Sj Mid1 ΔN1</i>	This study
<i>JK238</i>	<i>h leu1-32 pREP1-YFP-Sj Mid1 ΔN2</i>	This study
<i>JK246</i>	<i>h leu1-32 pREP1-YFP-Sj Mid1 ΔC1</i>	This study
<i>JK258</i>	<i>h leu1-32 pREP1-YFP-Sj Mid1 FL</i>	This study

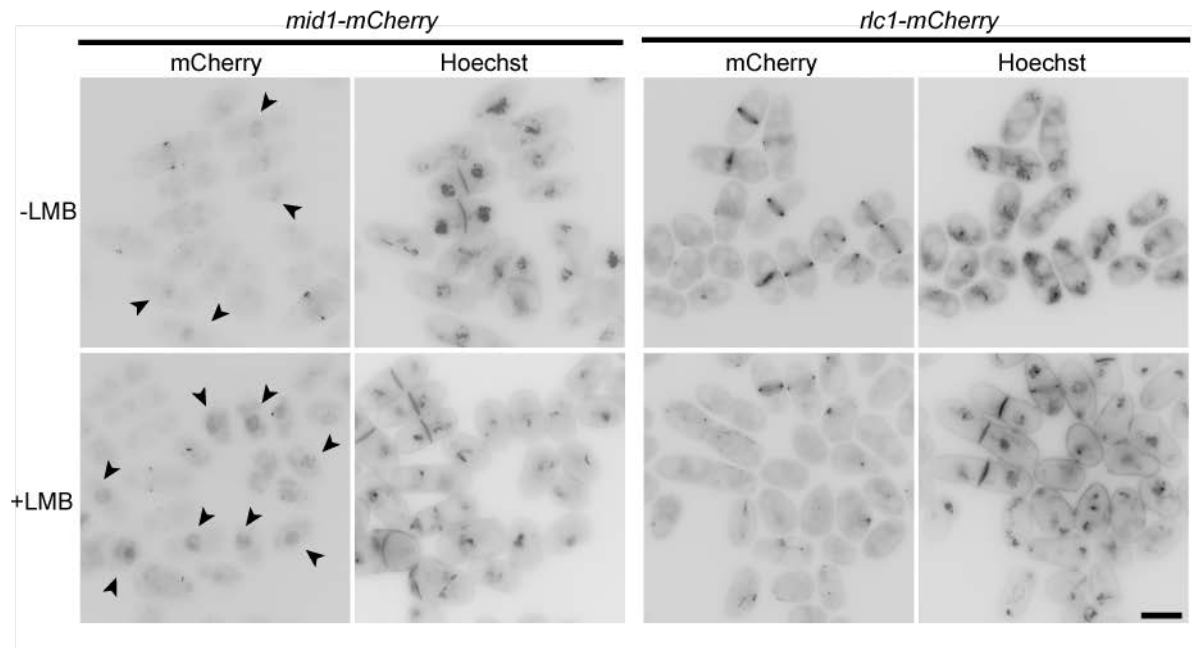
Table S2. *Schizosaccharomyces japonicus* strains used in this study

strains	genotype	source
NIG2021	<i>h</i> ⁹⁰	Prof. H. Niki
NIG2028	<i>h</i> ⁻	Prof. H. Niki
NIG8181	<i>h</i> ⁺ <i>cut11-GFP-natMX6</i>	Prof. H. Niki
JK27	<i>h</i> ⁻ <i>mid1-GFP-kanMX6</i>	This study
JK30	<i>h</i> ⁻ <i>mid1-mCherry-kanMX6</i>	This study
JK31	<i>h</i> ⁻ <i>rlc1-mCherry-kanMX6</i>	This study
JK56	<i>h</i> ⁹⁰ <i>cut11-GFP-natMX6</i>	This study
JK66	<i>h</i> ⁹⁰ <i>rlc1-mCherry-kanMX6</i>	This study
JK76	<i>h</i> ⁹⁰ <i>mid1-mCherry-kanMX6</i>	This study
JK92	<i>h</i> ⁻ <i>mid1-mCherry-kanMX6 cut11-GFP-natMX6</i>	This study
JK94	<i>h</i> ⁻ <i>rlc1-mCherry-kanMX6 cut11-GFP-natMX6</i>	This study
JK98	<i>h</i> ⁻ Δ <i>mid1::kanMX6 rlc1-mCherry-kanMX6</i>	This study
JK105	<i>h</i> ⁻ Δ <i>mid1::kanMX6</i>	This study
JK113	<i>h</i> ⁻ <i>mid1-GFP-kanMX6 rlc1-mCherry-kanMX6</i>	This study
JK117	<i>h</i> ⁻ <i>rlc1-GFP-kanMX6</i>	This study
JK133	<i>h</i> ⁻ <i>mid1-mCherry-kanMX6 rlc1-GFP-kanMX6</i>	This study
JK148	<i>h</i> ⁻ Δ <i>mid1::kanMX6 rlc1-mCherry-kanMX6</i> <i>cut11-GFP-natMX6</i>	This study
JK186	<i>h</i> ⁻ <i>rlc1-mCherry-kanMX6 sad1-mCherry-kanMX6</i>	This study
JK193	<i>h</i> ⁻ Δ <i>mid1::kanMX6 rlc1-mCherry-kanMX6</i> <i>sad1-mCherry-kanMX6</i>	This study
JK387	<i>h</i> ⁻ Δ <i>mid1::HA-Sj mid1</i> ⁺ - <i>GFP-kanMX6</i>	This study

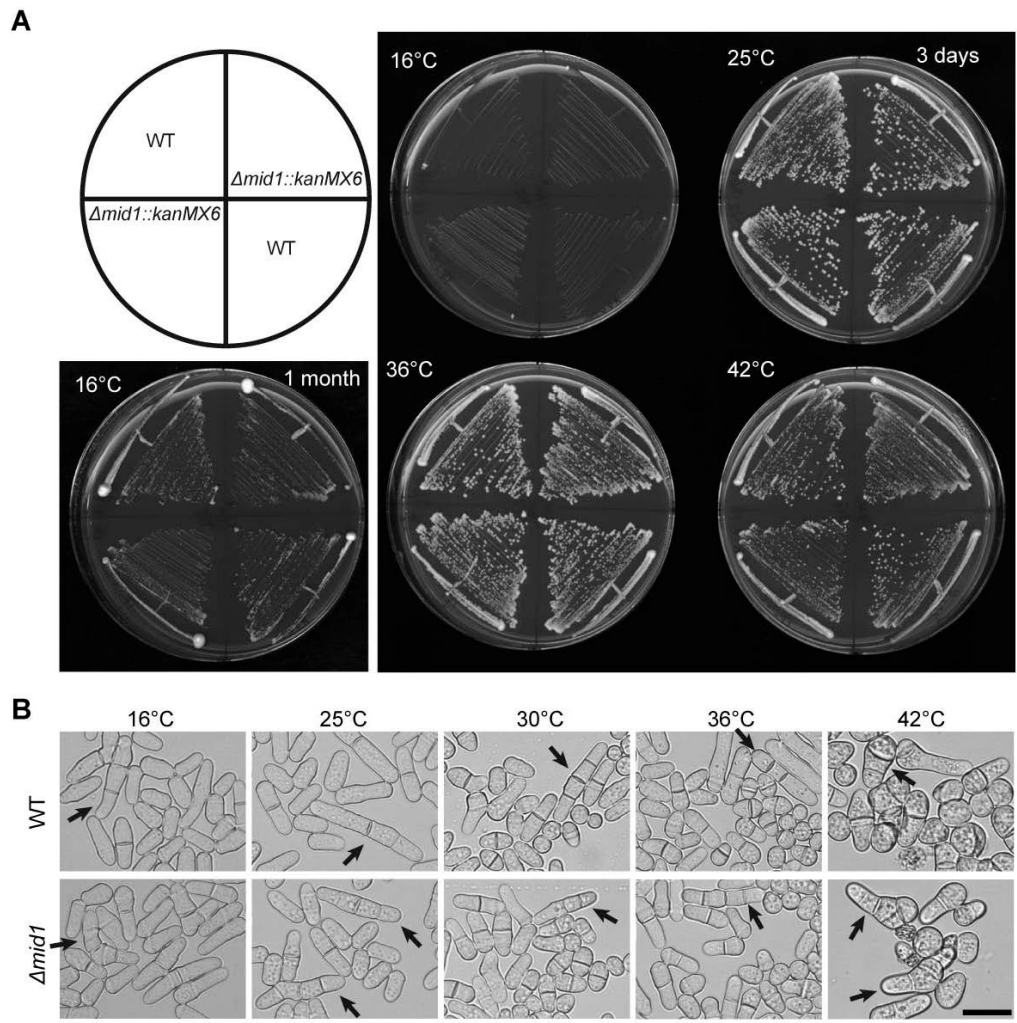
<i>JK392</i>	<i>h⁻ Δmid1::HA-Sp mid1⁺-GFP-kanMX6</i>	This study
<i>JK397</i>	<i>h⁻ Δmid1::HA-Sp mid1⁺-GFP-kanMX6</i>	This study
	<i>rlc1-mCherry-kanMX6 sad1-mCherry-kanMX6</i>	
<i>JK399</i>	<i>h⁻ Δmid1::HA-Sj mid1⁺-GFP-kanMX6</i>	This study
	<i>rlc1-mCherry-kanMX6 sad1-mCherry-kanMX6</i>	



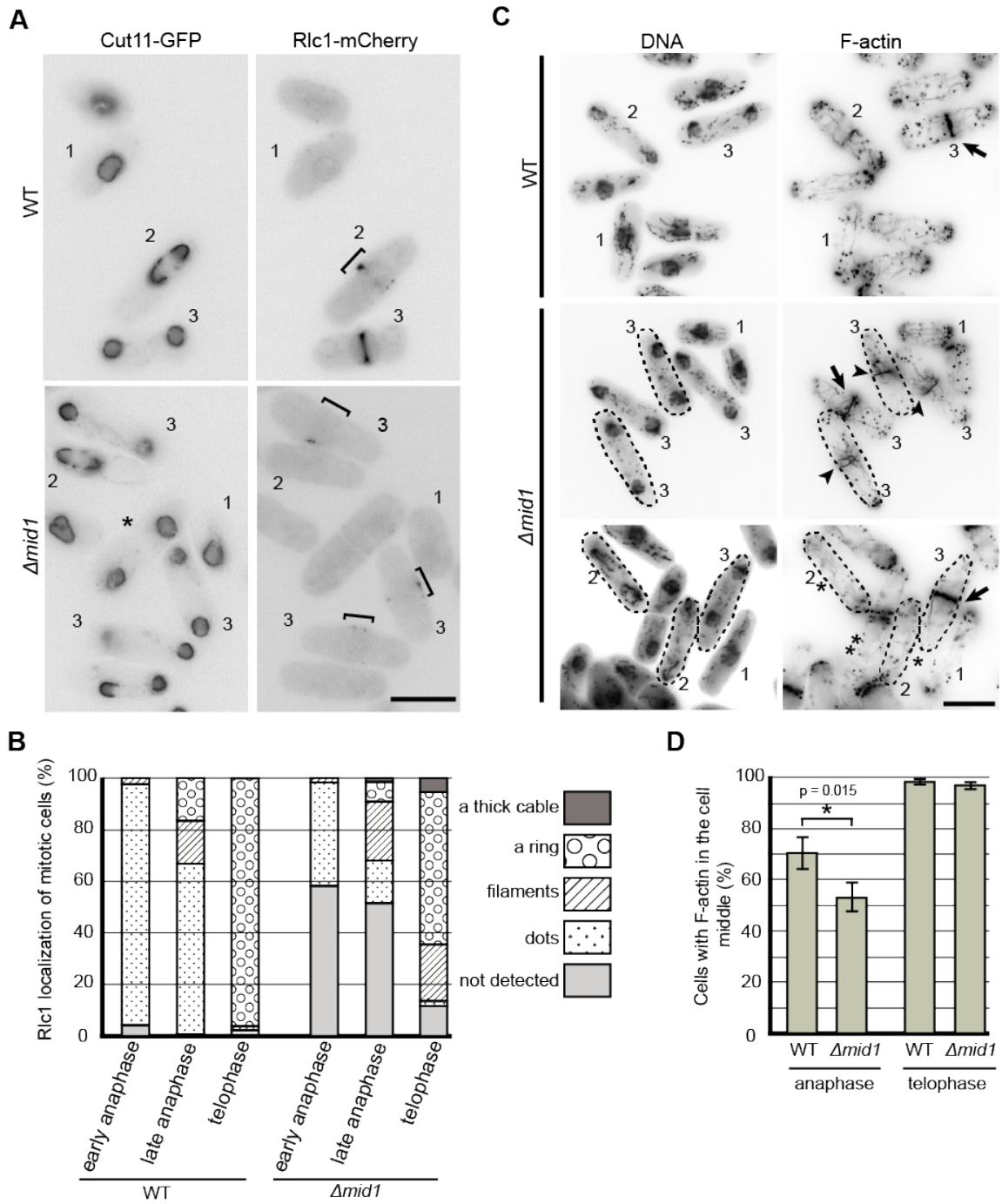
Yasuda *et al.* Figure 1



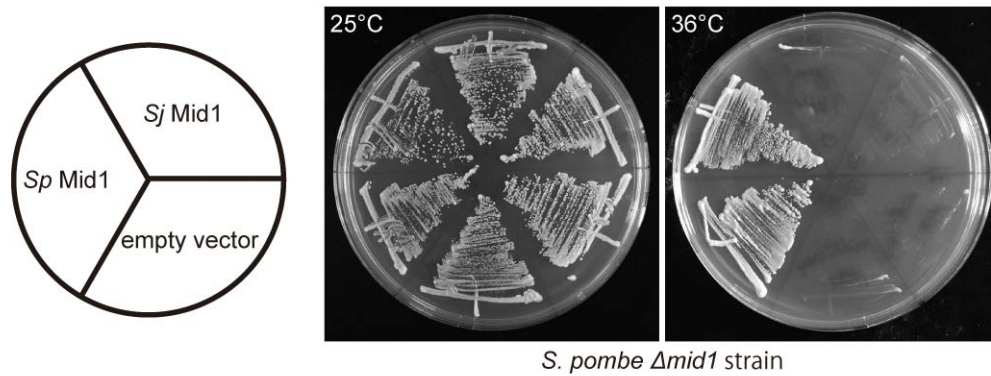
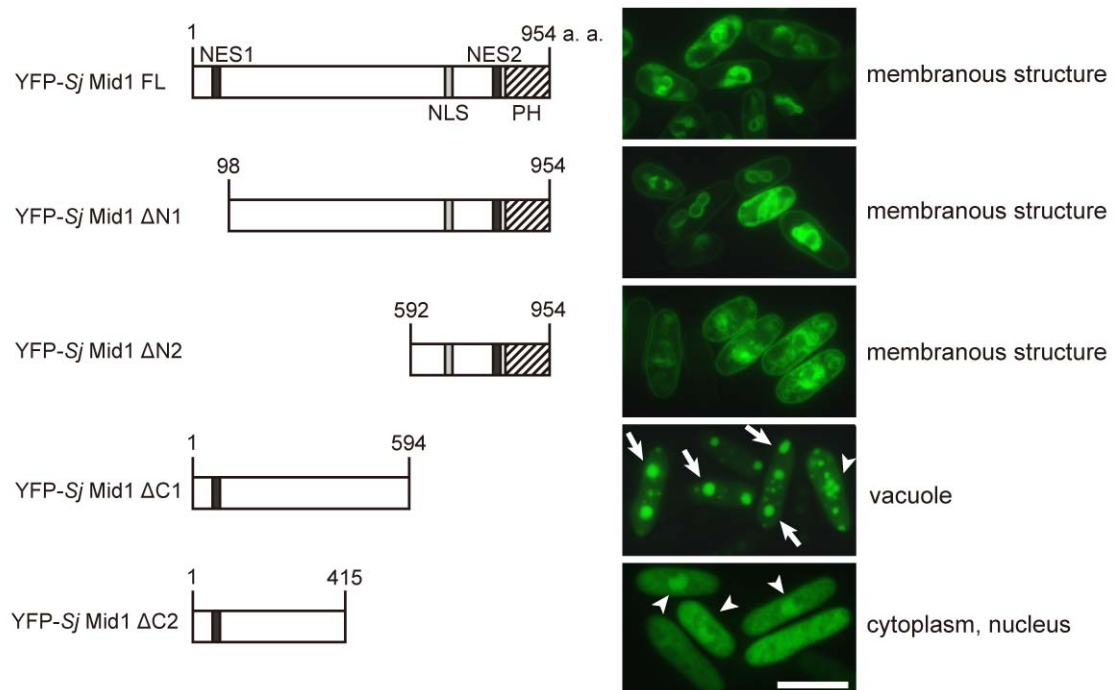
Yasuda *et al.*, Figure 2

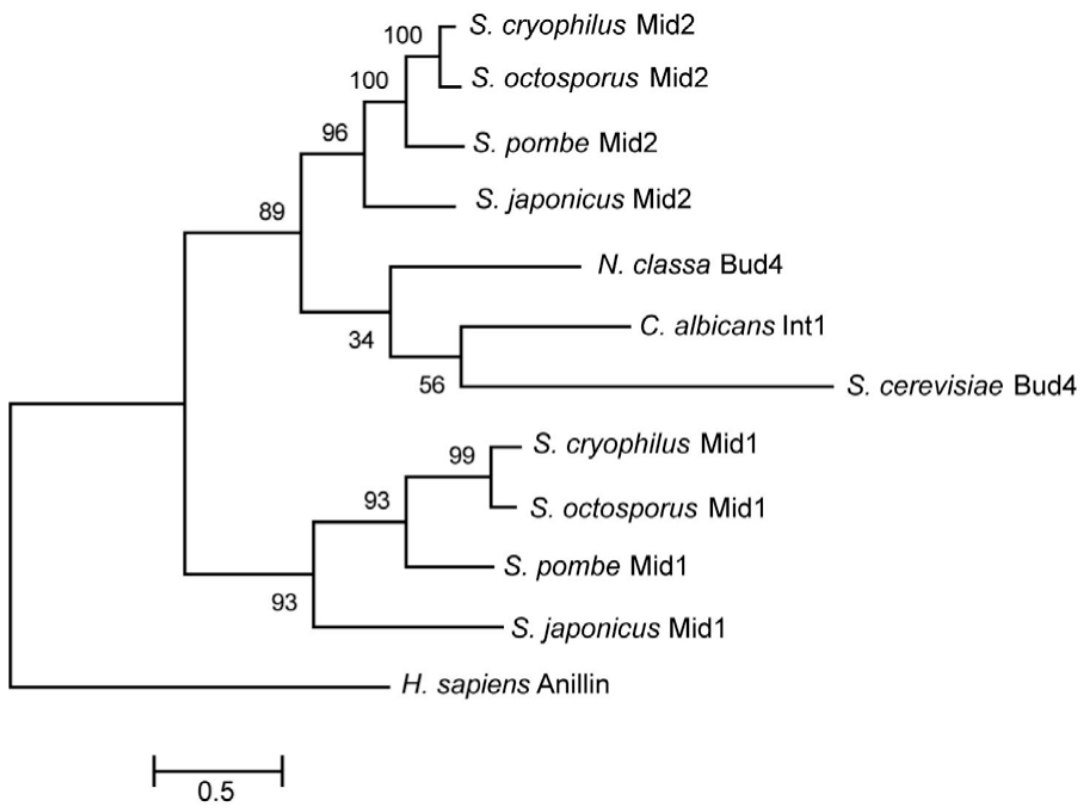


Yasuda *et al.*, Figure 3

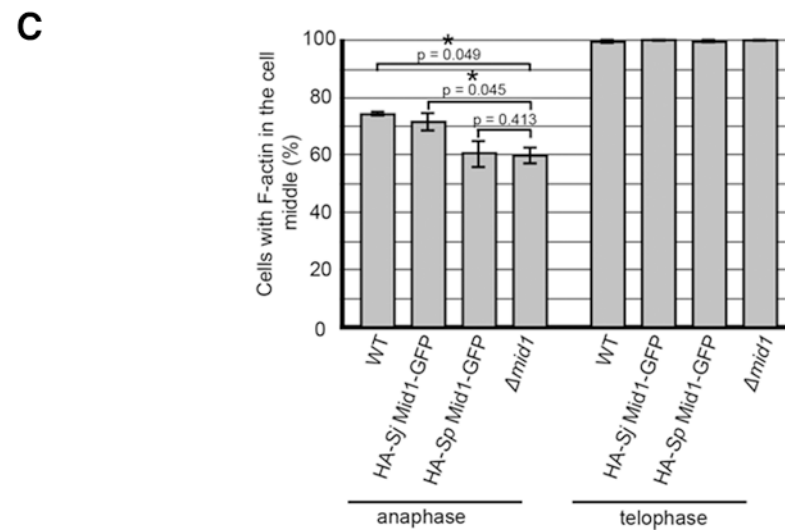
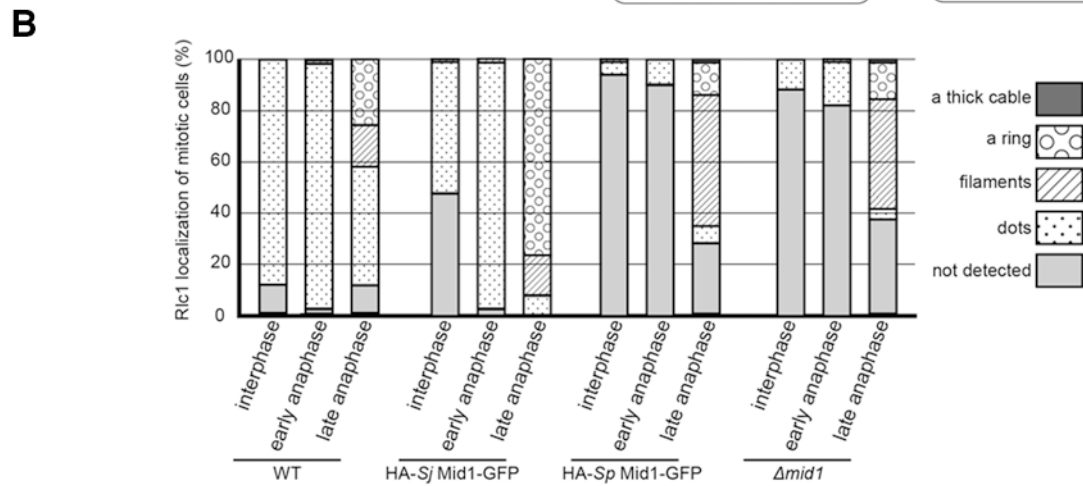
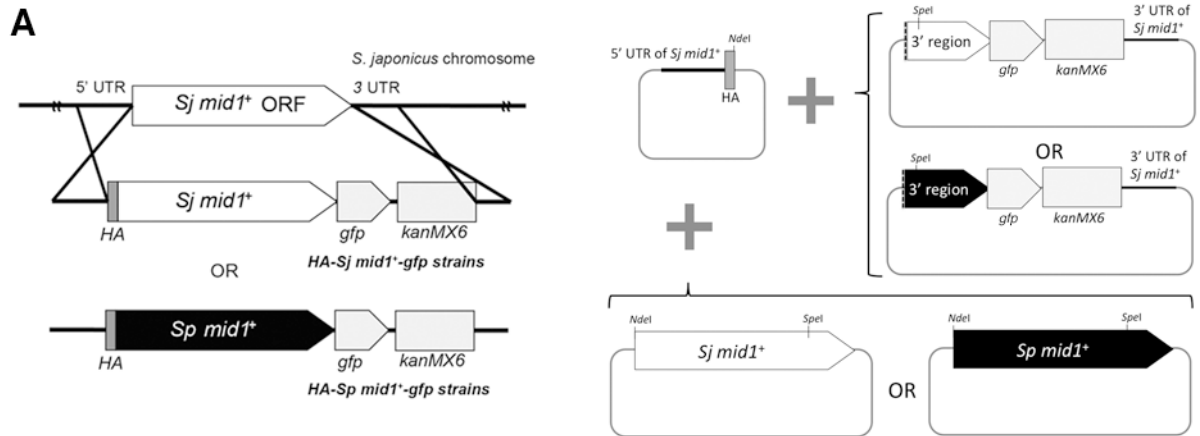


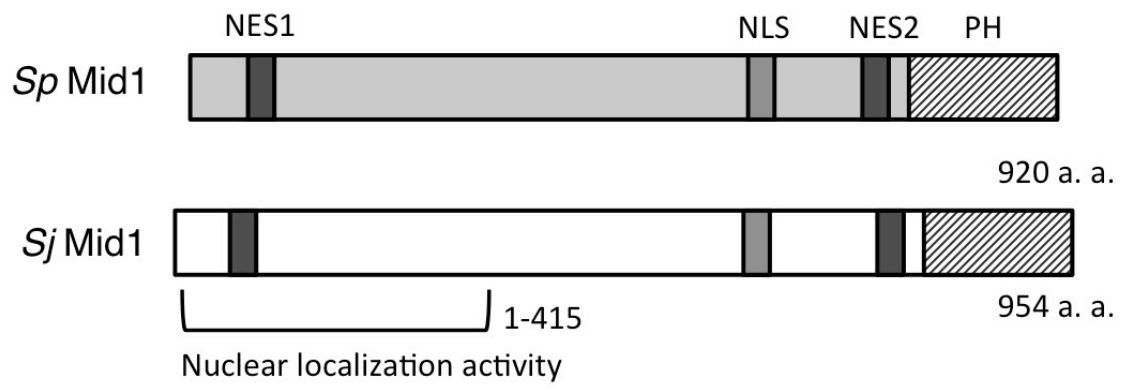
Yasuda *et al.* Figure 4

A**B**Yasuda *et al.* Figure 5



Yasuda *et al.* Supplemental Figure 1





Yasuda et al. Supplemental Figure 3